This article is published as part of the *Dalton Transactions* themed issue entitled:

Self-Assembly in Inorganic Chemistry

Guest Editors Paul Kruger and Thorri Gunnlaugsson

Published in issue 45, 2011 of *Dalton Transactions*

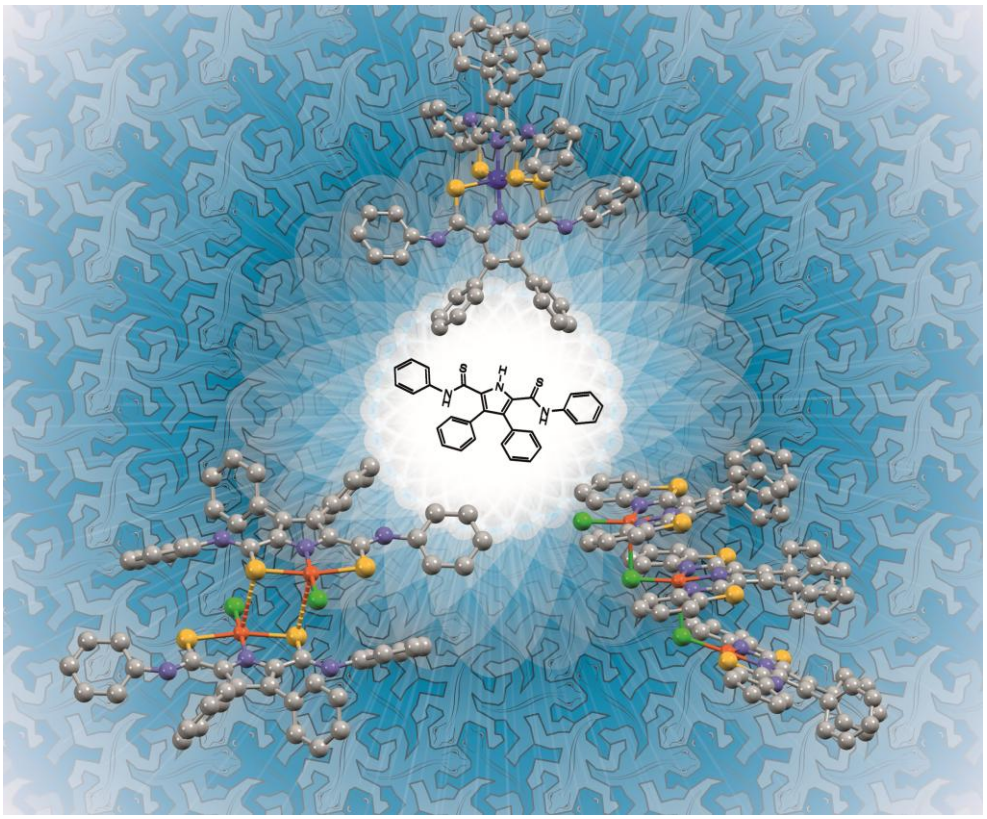

Image reproduced with permission of Mark Ogden

Articles in the issue include:

PERSPECTIVE:

ARTICLES:

Visit the *Dalton Transactions* website for more cutting-edge inorganic and organometallic research
www.rsc.org/dalton

Dalton Transactions

Dynamic Article Links

Cite this: *Dalton Trans.*, 2011, **40**, 12368

www.rsc.org/dalton

PAPER

Partial spin crossover behaviour in a dinuclear iron(II) triple helicate†

Rosanna J. Archer,[a] Chris S. Hawes,[a] Guy N. L. Jameson,[b] Vickie McKee,[c] Boujemaa Moubaraki,[d] Nicholas F. Chilton,[d] Keith S. Murray,[d] Wolfgang Schmitt[e] and Paul E. Kruger*[a]

Received 22nd July 2011, Accepted 26th September 2011
DOI: 10.1039/c1dt11381j

Reported herein are the synthesis, structural, magnetic and Mössbauer spectroscopic characterisation of a dinuclear Fe(II) triple helicate complex $[Fe_2(L)_3](ClO_4)_4.xH_2O$ (x = 1–4), **1**(H_2O), where L is a bis-bidentate imidazolimine ligand. Low temperature structural analysis (150 K) and Mössbauer spectroscopy (4.5 K) are consistent with one of the Fe(II) centres within the helicate being in the low spin (LS) state with the other being in the high-spin (HS) state resulting in a [LS:HS] species. However, Mössbauer spectroscopy (295 K) and variable temperature magnetic susceptibility measurements (4.5–300 K) reveal that **1**(H_2O) undergoes a reversible single step spin crossover at one Fe(II) centre at higher temperatures resulting in a [HS:HS] species. Indeed, the $T_{1/2}$(SCO) values at this Fe(II) centre also vary as the degree of hydration, x, within **1**(H_2O) changes from 1 to 4 and are centred between *ca.* 210 K–265 K, respectively. The dehydration/hydration cycle is reversible and the fully hydrated phase of **1**(H_2O) may be recovered on exposure to water vapour. This magnetic behaviour is in contrast to that observed in the related compound $[Fe_2(L)_3](ClO_4)_4\cdot 2MeCN$, **1**(MeCN), whereby fully reversible SCO was observed at each Fe(II) centre to give [LS:LS] species at low temperature and [HS:HS] species at higher temperatures. Reasons for this differing behaviour between **1**(H_2O) and **1**(MeCN) are discussed.

Introduction

Ongoing interest surrounds the synthesis and characterisation of spin crossover (SCO) complexes due to the many applications within which they may potentially find use, particularly as the active components in molecular memory, sensing and visual display devices.[1] SCO is best exemplified by mononuclear octahedral Fe(II) species where the low spin (LS; $S = 0$) to high spin (HS; $S = 2$) transition involves a dramatic change between diamagnetic and paramagnetic states along with significant concomitant structural and spectroscopic changes.[2] More recent studies have investigated higher nuclearity species and coordination polymers, and our understanding of SCO in these materials is rapidly evolving.[3,4]

We previously reported the use of dinuclear Fe(II) metallo-helicate complexes as molecular hosts, and studied binding events within their intra-helical cavities, with the view of ultimately including SCO within related metallo-helicate complexes.[5] This would make them very attractive materials for the recognition of guest molecules using the SCO magnetic, structural and spectroscopic signatures to indicate any binding event. To achieve this first requires a thorough study of SCO in metallo-helicate complexes however relatively few reports detail such phenomena in these species.[6] We recently reported that a dinuclear triple-helicate complex, $[Fe_2(L)_3](ClO_4)_4\cdot 2MeCN$, **1**(MeCN), where L is a bis-bidentate imidazolimine ligand, showed complete switching between the LS to HS states at each Fe(II) centre (HS:HS–LS:LS) under both temperature and light control (LIESST).[7] Encouraged by these results we report here the synthesis, structural, magnetic and Mössbauer spectroscopic characterisation of a closely related water solvated (structural) analogue, $[Fe_2(L)_3](ClO_4)_4\cdot xH_2O$ (x = 1–4), **1**(H_2O), and compare and contrast its differing behaviour to that of the acetonitrile solvated analogue, **1**(MeCN).

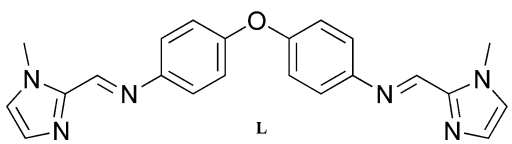

L

Results and discussion

Synthesis and characterisation

Complex **1**(H_2O) was obtained by adding a methanolic solution of $Fe(ClO_4)_2\cdot 6H_2O$ dropwise to a methanolic solution of **L** in

[a]*Department of Chemistry, University of Canterbury, Private Bag 4800, Christchurch, 8041, New Zealand. E-mail: paul.kruger@canterbury.ac.nz*
[b]*Department of Chemistry & MacDiarmid Institute for Advanced Materials & Nanotechnology, University of Otago, PO Box 56, Dunedin, 9054, New Zealand*
[c]*Department of Chemistry, Loughborough University, Loughborough, Leicestershire, LE11 3TU, England*
[d]*School of Chemistry, Monash University, Clayton, Victoria, 3800, Australia*
[e]*University of Dublin, Trinity College, School of Chemistry & CRANN, Dublin 2, Ireland*

† Electronic supplementary information (ESI) available: Experimental details, selected distances and angles for **1**(H_2O), crystallographic packing diagrams and parameters, TGA and ESMS data. CCDC reference number 836247. For ESI and crystallographic data in CIF or other electronic format see DOI: 10.1039/c1dt11381j

2 : 3 stoichiometry. A dark orange precipitate immediately formed which was subsequently recrystallised from MeCN following the slow diffusion of diethylether to yield thin red lath crystals. The elemental data are consistent with the formation of dinuclear species of general formula $[Fe_2L_3]^{4+}$ and this composition was further confirmed by the electrospray mass spectrum (ESMS). Indeed, ESMS displayed peaks characteristic of $[Fe_2L_3]^{4+}$ ions in solution as a peak fitting the tetra-cation was observed (see ESI†). The crystals of $[Fe_2(L)_3](ClO_4)_4 \cdot 1.5H_2O$, enabled their structure to be determined by single crystal X-ray diffraction, Fig. 1.‡

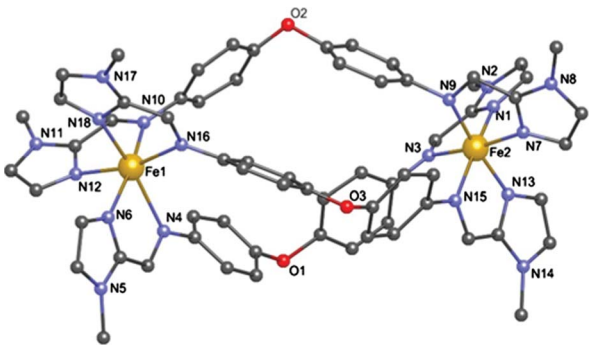

Fig. 1 Molecular structure of **1**(H_2O) at 150 K. Hydrogen atoms, perchlorate anions and water molecules have been omitted for clarity.

X-Ray crystal structure of 1(H_2O)

As anticipated, the structure of **1**(H_2O) consists of a dinuclear triple helicate within which the Fe(II) are in pseudo-octahedral environments bound to three imidazolimine units from three different ligands. Each ligand binds to two Fe(II) centres, yielding an intra-helical Fe···Fe separation of 11.45 Å (inter-helical Fe1···Fe2 distance is shorter, 8.95 Å). Four of the six aryl rings within the helicate participate in intramolecular edge-to-face CH···π bonding although the increased CH···π distance and contracted angles indicate a weaker interaction than the comparable interactions observed in **1**(MeCN) (see Table S1, Fig. S1†). Indeed, the subtle differences in these intramolecular CH···π interactions in **1**(H_2O) *cf.* **1**(MeCN) results in a flattening out of the ligand strands and enables one strand within the helicate to participate in an intermolecular face-to-face π···π interaction with an adjacent helicate, Fig. 2. In contrast, there were no such intermolecular contacts observed between adjacent helicates in **1**(MeCN) (see Fig. S2†). The dissimilarity observed for the Fe–N bond distances and bite angles around Fe1 and Fe2 illustrates that at 150 K Fe1 is in the HS state whereas Fe2 is in the LS state, Table 1. This is in contrast to the corresponding structural data for **1**(MeCN) which showed that each Fe-centre was in the LS configuration at 150 K. We therefore studied the magnetic susceptibility and Mössbauer spectroscopy of **1**(H_2O) as a function of temperature to identify any SCO behaviour and to compare and contrast this with the SCO behaviour found in **1**(MeCN).

‡ Crystal data for **1**(H_2O): $C_{66}H_{60}Cl_4Fe_2N_{18}O_{20.5}$, $M = 1686.82$, monoclinic, $a = 14.82(4)$ Å, $b = 27.22(8)$ Å, $c = 18.98(6)$ Å, $\beta = 107.88(4)°$, $V = 7284(36)$ Å^3, $\lambda = 0.77490$ Å, $T = 150(2)$K, space group $P2_1/c$, $Z = 4$, 37303 reflections measured, 7330 independent reflections ($R_{int} = 0.5358$). The final R_1 values were 0.1242 ($I > 2\sigma(I)$). The final $wR(F^2)$ values were 0.2600 ($I > 2\sigma(I)$). The final R_1 values were 0.3104 (all data). The final $wR(F^2)$ values were 0.3435 (all data).[18] Data were measured at ALS station 11.3.1.

Table 1 Selected bond lengths [Å] and bite angles [°] for **1**(H_2O) at 150 K

	$Fe–N_{imidazole}$ [Å]		$Fe–N_{imine}$ [Å]		Bite angle [°]
Fe1	N18	2.130(16)	N16	2.168(14)	78.1(6)
	N12	2.116(14)	N10	2.255(17)	76.5(6)
	N6	2.132(17)	N4	2.287(16)	76.7(6)
Fe2	N7	1.948(12)	N9	1.984(16)	79.7(6)
	N13	1.931(16)	N15	1.984(17)	80.8(7)
	N1	1.936(16)	N3	1.965(14)	80.2(6)

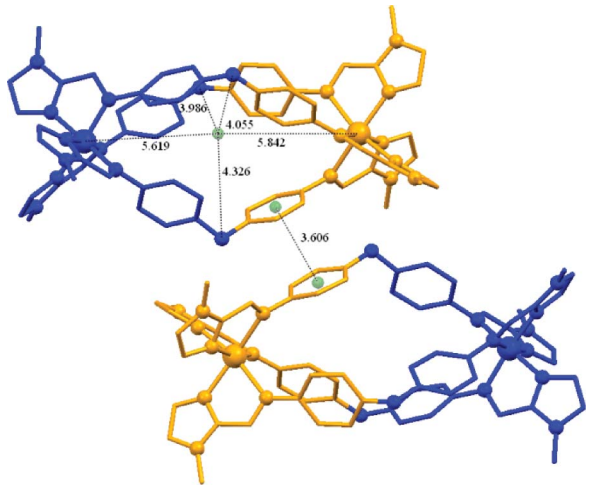

Fig. 2 Packing diagram for **1**(H_2O) showing the intermolecular π–π-interactions between adjacent helicate species and pertinent intra-helical distances as dashed lines. Helicate 'halves' containing HS Fe1 and LS Fe2 are coloured orange and blue, respectively. Hydrogen atoms, perchlorate anions, and water molecules are omitted for clarity.

Magnetic and Mössbauer spectroscopic properties of 1(H_2O)

Variable temperature magnetic susceptibility measurements were performed upon a crystalline sample of **1**(H_2O) over a temperature range of 2–300 K. Plots of μ_{eff} *vs.* T are shown in Fig. 3. Focusing on the first cycle (open circles in Fig. 3), between 2–300 K, the plot is typical of a 'half' spin crossover with a broad spin transition, from [HS(Fe1)–LS(Fe2)] to [HS–HS] states, and occurs between ~210 and 300 K with $T_{1/2}$ ~265 K. The 'full' [HS–HS] state is not quite reached at 300 K. The high value (5.54 μ_B per Fe) is indicative of orbital degeneracy in this formally $^5T_{2g}$ system. The return run, from 300–2 K, now shows a [HS–HS] region between 300 to ~260 K and a gradual transition that rejoins the [HS–LS] plateau at ~180 K. The [HS–LS] plateau covers a wide region between ~200 to 50 K, with μ_{eff} = 4.14 μ_B per Fe, then shows a rapid decrease to 3.25 μ_B, at 5 K, due to zero-field splitting of the quintet (HS) state arising from the [HS–LS] form. The second cycle, 2–300–2 K, (central red pair of lines, Fig. 3), measured on the same sample after it had undergone the first cycle in the SQUID sample chamber, shows a further move to lower temperature for the [HS–LS] to [HS–HS] transition ($T_{1/2}$ ~240 K). It appears to show thermal hysteresis (ΔT ~ 12 K), but, as in the first cycle, probably involves partial loss of solvate water. This is further confirmed by making measurements on the same

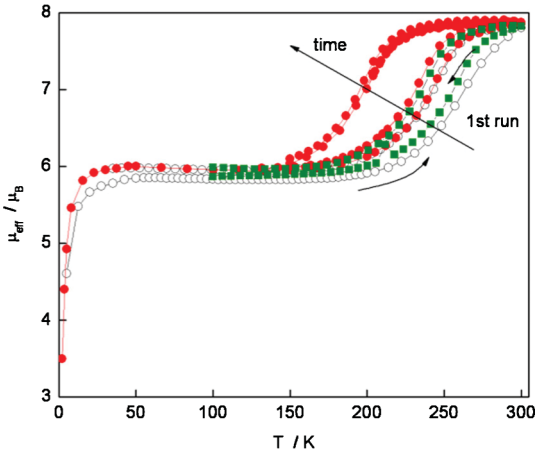

Fig. 3 Plot of the effective magnetic moment per dinuclear helicate *vs.* T for **1**(H_2O). The open circles trace the 1st cycle (2–300–2 K) with the arrows indicating the direction of the 1st and 2nd runs. The central filled red circles trace the 2nd cycle, and the exterior filled red circles trace the 3rd cycle (these cycles were recorded over a period of hours and the diagonal arrow indicates the effect of dehydration and the passage of time). The filled green squares are the 4th cycle (100–300–100 K) recorded after the sample had been allowed to sit in air (within the gelatine capsule) for some weeks and demonstrate the recovery of the rehydrated sample.

sample after it had sat, under the vacuum in the sample chamber, at 300 K for 2 h, as shown in the left, red plot of Fig. 3. The 'up' and 'down' plots are now very close at the spin transition, with $T_{1/2}$ of ~200 K. The rest of the [HS–LS] plateau and the low temperature rapid decrease in magnetic moment are the same as before. The sample is now; after 2 h at 300 K, desolvated and this is corroborated by TGA measurements which show the loss of lattice water molecules, at ambient pressure, is complete by *ca.* 370 K (see Fig S3†). Interestingly, allowing samples from either the magnetic or TGA measurements to sit under ambient conditions for a period of days/weeks and subsequently repeating either measurement shows that these 'aged' samples almost recover the profiles of the pristine samples as evidenced by the plots shown in green in Fig. 3 (and a similar weight loss trace in the TGA, Fig. S3†), which is consistent with the recovery of the hydrated phase.

When considering the magnetic susceptibility data in relation to the Mössbauer spectral results (Fig. 4; Table 2), then the (poorly resolved) room temperature spectrum suggests that some LS form remains. At 295 K the sample shows what at first inspection looks like a single quadrupole doublet. Closer inspection suggests that there are, in fact, two species in an approximately 3 : 1 ratio, which are most likely HS and LS Fe(II). This is not uncommon in such spin crossover materials and, further, inspection of the magnetic plot (Fig. 3) shows that 295 K lies towards the top of the spin transition, rather than fully in the [HS–HS] region. The 1 : 1 HS to LS area ratio at 4.5 K is in good agreement with the magnetic and crystallographic data, being due to the HS (Fe1) and LS (Fe2) centres within each dinuclear helicate molecule and not due to 1 : 1 mixture of [LS–LS] and [HS–HS] molecules. A further point of interest is the large change in the Mössbauer parameters for the HS site between 295 and 4.5 K. The increase in the isomer shift as the temperature is decreased is due to a second order Doppler shift;[8] while the large increase in the quadrupole splitting is commonly observed in spin crossover compounds.[4,9] The size of

Table 2 Mössbauer parameters for **1**(H_2O) at 4.5 and 295 K

T (K)	Spin State	δ (mm s^{-1})	ΔE_Q (mm s^{-1})	Γ_L (mm s^{-1})	Γ_R(mm s^{-1})	I (%)
4.5	HS	1.11	2.49	0.27	0.42	50
	LS	0.45	0.47	0.26	0.26	50
295	HS	0.92	1.48	0.55	0.55	75
	LS	0.34	0	0.35	0.35	25

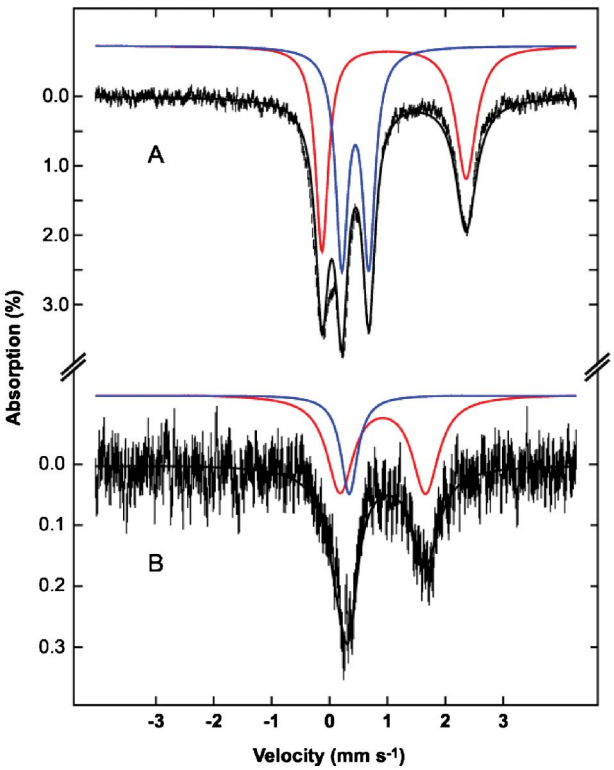

Fig. 4 Mössbauer spectra of **1**(H_2O) at 4.5 K (A) and 295 K (B). The experimental data were fitted with the parameters detailed in Table 2 with the HS and LS Fe(II) fractions in red and blue, respectively.

the change in ΔE_Q here, however, suggests a modification of the coordination geometry around Fe1 as the temperature is lowered, although the exact nature of this change is difficult to identify.

The origin of the [HS–LS] plateau in the magnetism, and the causes thereof at a molecular level, are intriguing but difficult to assign with any certainty. Clearly, decreasing temperature does not cause the full conversion of the [HS–HS] to [LS–LS] state as was the case in **1**(MeCN). The question is posed as to why the [HS–LS] structure is so stable in **1**(H_2O). Perusal of the environments surrounding the Fe-coordination spheres within **1**(H_2O) and **1**(MeCN) reveals some dissimilarity between the two that might lead to their differing behaviours (see Fig. S1 and S2 and Table S1†). The intramolecular interactions within the helicate are different, as discussed earlier, as are the intermolecular interactions seen within the crystal packing (see Fig. S2†). The most striking difference between the two complexes is the presence of the intermolecular face-to-face $\pi\cdots\pi$ interaction between HS–Fe1 ends within **1**(H_2O), which allows adjacent helicates to pair-up, Fig. 2. The separation between helicates throughout the crystal lattice involving the other ligand strands are further distant (*ca.* >4.1 Å) and are therefore not considered to have as

significant influence on the Fe spin-states. Likewise, there are no close intermolecular interactions between helicates in **1**(MeCN). Perhaps it is the π···π interaction involving the HS-ends in **1**(H_2O) that prevents the helicates from undergoing full SCO to yield the [LS–LS] state, as transition to the LS state at Fe1 would contract the coordination sphere and potentially reduce this favourable π···π interaction.

The dependence of $T_{1/2}$(SCO) of Fe2 upon the degree of hydration also warrants discussion.[10] The efflux/influx of water comes without the loss of crystallinity as the structure of **1**(H_2O) was determined upon 'aged' crystals where no precaution was made to prevent water loss *i.e.* they were stored dry and absent from their mother liquor. It is tempting to associate this observation with the four partially-occupied water sites located in the crystallography. These are linked to the perchlorate counter ions in a discrete H-bonded chain which would have stoichiometry $(ClO_4)_2(H_2O)_4$ if all the water sites were fully occupied (Fig S5†). TGA experiments show that water loss is immediate at RT and that the complex is stable up to a minimum of 373 K. Clearly this process is reversible as the magnetic behaviour of the aged samples following sample rehydration essentially retraces that of the pristine sample. Inspection of the crystal packing reveals a viable route for water molecule egress through channels that perforate the crystal along the *c*-axis. Indeed, the space within which the water molecules reside accounts for *ca.* 9% void volume in the crystal.[11] Following dehydration it becomes easier for the complex to attain the [HS–HS] state as $T_{1/2}$(SCO) for Fe2 moves progressively to lower temperatures. The exact reason for this is difficult to identify but presumably Fe2, in the absence of the water molecules of crystallisation, is less sterically encumbered by lattice constraints and more easily enters the HS state.

To gain some knowledge of the thermodynamics and speciation of the spin transition in solid **1**(H_2O) (in the absence of heat capacity or differential scanning calorimetry measurements) we have made a van't Hoff analysis and fitted the ln$K$ *vs.* $1/T$ data (see ESI for details).[12] The K values were for the 'half' spin transition equilibrium (eqn (1)) and extracted from the $\mu_{eff}/\chi_M T$ data in Fig. 3 using the data for the various cycles; see ESI† for details.

$$[Fe(LS)Fe(HS)]^{4+} \overset{K}{\longleftrightarrow} [Fe(HS)Fe(HS)]^{4+} \quad (1)$$

The first cycle did not quite reach the HS–HS state at 300 K and thus there are only a few points on the spin transition showing linearity such that the intercept ($\Delta S/R$) yielded a very high ΔS of 200(30) J mol^{-1} K^{-1} with ΔH = 49(10) kJ mol^{-1}. Much more reliable are runs 2–4, appropriate to desolvated forms, that gave good linearity and the same thermodynamic parameter values, *viz.* ΔH = 17(2) kJ mol^{-1} and ΔS = 100(9) J mol^{-1} K^{-1}. The 4th cycle, for the (partially) resolvated form gives parameters approaching those for the first cycle; ΔH = 27(2) kJ mol^{-1} and ΔS = 148(10) J mol^{-1} K^{-1}. These parameter values are reasonably typical of Fe(II) spin crossover compounds including dinuclear systems. For example, in the dinuclear bipyrimidine (bpym)-bridged systems, that have quite different ligand donors and coordination geometry to **1**(H_2O), the complex [Fe(bithiazoline)-$(NCS)_2]_2$(μ-bpym) shows a 2-step transition,[13] yielding (from heat capacity) ΔH = 5.4(0.5) kJ mol^{-1} and ΔS = 41(3) J mol^{-1} K^{-1} for the step equivalent to eqn (1). The half-crossover complex [Fe(bpym)$(NCSe)_2]_2$(μ-bpym) showed (from heat capacity) ΔH ~15 kJ mol^{-1} and ΔS = 25(3) J mol^{-1} K^{-1}.[14] A series of pyrazolate-bridged dinuclear complexes, also with different donor sets and Fe(II) geometry to the present compound, yielded ΔH = 6 to 13 kJ mol^{-1} and ΔS = 47 to 65 J mol^{-1} K^{-1} for the full LS–LS to HS–HS transition.[15] Most relevant to the present helicate complex is a related dinuclear triple-helicate that showed a partial crossover (very much on the LS side), a van't Hoff analysis of solution susceptibilities being used that defined K for LS–LS to HS–HS. It showed ΔH = 31.1(4) kJ mol^{-1} and ΔS = 76(3) J mol^{-1} K^{-1}.[6g] These are not too dissimilar to the values deduced for **1**(H_2O) when allowing for the uncertainties involved in the solution susceptibility measurements.[6g] All of the entropy changes quoted above, particularly for **1**(H_2O), are bigger than that expected from a change in spin state alone, *viz.* $\Delta S = R\ln[(2S+1)_{HS}/(2S+1)_{LS}]$ = 13.4 J mol^{-1} K^{-1}, a feature commonly noted with the excess in ΔS being ascribed to vibrational contributions deriving from stretching and other modes at the Fe(II) coordination centres.

Conclusions

The present compound, **1**(H_2O), joins a small but growing group of dinuclear [Fe(II)–Fe(II)] spin crossover complexes that behave similarly in stabilising the [HS–LS] form and showing half spin transitions.[16] Such compounds possess shorter Fe···Fe separations, and more rigid covalent bridge bonding than does the present helicate compound. A common feature in most though is that the site symmetry of the two Fe centres is different even in the HS–HS forms. Moreover, **1**(H_2O) is a new member of a family of complexes that show interesting and variable SCO that is dependent upon the reversible incorporation of guest species within their crystal lattices.[10] We are currently extending this family of complexes to include different counter-anions, ligand types, solvents of crystallisation and other nuclearity and will report upon these examples in the future.

Experimental

General

All reagents and solvents were purchased from commercial sources (Aldrich) or local solvent suppliers and used without further purification. ^{1}H (^{13}C) NMR spectra were acquired on an INOVA 500 spectrometer operating at 500 (125) MHz and referenced to the residual proton shifts in the internal deuterated solvent. Chemical analyses were performed at the Campbell Microanalytical Laboratory, University of Otago, Dunedin, New Zealand. Mass spectra were recorded on a Bruker maXis 4G electrospray instrument. Infrared spectra were carried out using a Perkin Elmer Spectrum One FTIR spectrometer in the range 400–4000 cm^{-1}. Solid samples were analysed *via* diffuse reflectance in ground KBr. The following abbreviations have been used: br (broad); s (strong). Thermal analyses were carried out using an Alphatech SDT Q600 TGA/DSC apparatus. All samples were heated on alumina crucibles under nitrogen flow of 100 cm^3 min^{-1}.

The magnetic susceptibilities were measured using a Quantum Design Squid magnetometer, PPMS 5, at a dc field of 1 T, with the samples (*ca.* 10 mg) contained in gelatin capsules held at the centre of a drinking straw that was fixed to the end of the sample rod. Ligand diamagnetic corrections were obtained using Pascal's constants. ^{57}Fe Mössbauer spectra were recorded at the University

of Otago (GNL). Approximately 10–35 mg of sample was placed in a nylon sample holder (12.8 mm diameter, 1.6 mm thickness) with Kapton windows. Mössbauer spectra were measured on a Mössbauer spectrometer from SEE Co. (Science Engineering & Education Co., MN) equipped with a closed cycle refrigerator system from Janis Research Co. and SHI (Sumitomo Heavy Industries Ltd.). Data were collected in constant acceleration mode in transmission geometry with an applied field of 47 mT parallel to the γ-rays. The zero velocity of the Mössbauer spectra refers to the centroid of the room temperature spectrum of a 25 μm metallic iron foil. Analysis of the spectra was conducted using the WMOSS program (SEE Co., formerly WEB Research Co. Edina, MN).

Single crystal data and experimental details for **1**(H_2O) are summarised in Table S2.† The single crystal analysis was performed at 150(2) K on line 11.3.1 of the Advanced Light Source. All of the crystals were very thin (curly!) laths, several were tried and each gave very broad, streaky, low intensity peaks but the same unit cell. The structure was solved by direct methods and refined on F^2. All the non-H atoms were refined anisotropically (using SIMU and DELU restraints) and H atoms were inserted at calculated positions except for those of the partial occupancy water molecules, which were not included in the model.[18] Due to the very weak data, the statistics (R_{int} *etc.*) are poor but, nevertheless the refinement behaved reasonably well. It converged at R_1 = 12.4% for data out to 2θ = 45°, higher angle data were not used in the refinement as there was no significant intensity present. Unsurprisingly, checkcif produces a range of alerts for this structure; these are all due to the basic problem of the very weak data but, given that the data were collected on a synchrotron, there is no real prospect of an improved data set. However, the cell and structure are basically correct, the geometry and bond distances are all in the expected ranges and the differences between the two iron sites are clear-cut (see Table S3†). Assignment of the solvate molecules as water is supported by the characterisation studies of the bulk sample and also by the observation that they make a reasonable (and finite) H-bonded unit with the perchlorate anions (Fig. S5†). O1 w and O2 w were refined with 50% occupancy, O3 w and O4 w with 25% occupancy. Partial loss of water molecules may be the cause of the broad diffraction peaks. Selected bond lengths [Å] and angles [°] for **1**(H_2O) are given in Table S3.†

Crystallographic data (excluding structure factors) for **1**(H_2O) has been deposited with the Cambridge Crystallographic Data Centre as supplementary publication CCDC Number: 836247.† Copies of the data can be obtained, free of charge, on application to CCDC, 12 Union Road, Cambridge CB2 1EZ, UK: http://www.ccdc.cam.ac.uk/cgi-bin/catreq.cgi, E-mail: data_request@ccdc.cam.ac.uk, or fax: +44 1223 336033

Synthesis of L

Following adapted procedures from those previously reported.[17] 1-Methyl-2-imidazolecarboxaldehyde (220 mg, 1.96 mmol) and 4,4′-oxydianiline (200 mg, 0.97 mmol) were stirred in MeOH (10 ml) for 18 h. The clear solution was evaporated to dryness; the oil obtained dissolved in CH_2Cl_2 and dried over $MgSO_4$, filtered and the solvent removed under vacuum. The residue obtained was recrystallised from MeCN and the off-white powder collected by filtration. Yield: 215 mg, 58%; mp: 154 °C; $C_{22}H_{20}N_6O$ requires: C 68.72, H 5.25, N 21.87, found: C 68.47, H 5.44, N 21.53%; ^{1}H NMR [$(CD_3)_2SO$, 500 MHz, 293 K]: δ = 8.52 (s, 1H, H3), 7.43 (s, 1H, H1), 7.37 (d, 2H, J = 8.8 Hz, H5), 7.16 (s, 1H, H2), 7.08 (d, 2H, J = 8.8 Hz, H4), 4.05 (s, 3H, Me); ^{13}C NMR [$(CD_3)_2SO$, 125 MHz, 293 K]: δ = 155.3 (Q), 150.5, 146.3 (Q), 142.8 (Q), 129.7, 126.5, 122.8, 119.4, 35.2.

Synthesis of $[Fe_2(L)_3][ClO_4]_4 \cdot xH_2O$ (x = 1–4), 1(H_2O)

Ligand L (92 mg, 0.24 mmol) was dissolved in MeOH (5 ml) and a MeOH solution (5 ml) of $[Fe(ClO_4)_2 \cdot 6H_2O]$ (60 mg, 0.17 mmol) was added dropwise. A dark-orange precipitate formed instantly. The reaction mixture was stirred at RT for 15 min and the product collected by filtration and recrystallised from MeCN following the slow diffusion of diethylether, and the thin red-laths were collected and air dried. Yield: 90 mg, 68%; $Fe_2C_{66}H_{60}N_{18}O_{19}Cl_4 \cdot 3H_2O$ requires: C, 46.17; H, 3.88; N, 14.69%. Found: C, 46.25; H, 3.79; N, 14.58%; MS-ESI m/z (MeCN): Calculated for $[Fe_2C_{66}H_{60}N_{18}O_3]^{4+}$ = 316.0944 $[Fe_2L_3]^{4+}$. Found = 316.0958. IR (KBr) cm^{-1} 3511 br, 1628, 1495 s, 1448, 1328, 1295, 1243 s, 1080 s, 927, 903, 865, 776, 664, 593, 532, 508, 473, 455.

Caution! No problems were encountered in this study when using the perchlorate derivatives described. However, suitable care must be taken when handling such potentially explosive materials.

Acknowledgements

The authors thank the University of Canterbury (Scholarship to CSH); the Royal Society of New Zealand Marsden Fund (PEK); the Science Foundation Ireland (WS; 08/IN.1/I2047), and; the Australian Research Council (KSM) for financial support. VMcK thanks the University of Canterbury for the award of an Erskine Visiting fellowship. The Advanced Light Source is supported by the Director, Office of Science, Office of Basic Energy Sciences, of the U.S. Department of Energy under Contract No. DE-AC02-05CH11231. The authors also thank Dr Anthea Lees for helpful discussion.

Notes and references

1 *Spin Crossover in Transition Metal Compounds I–III*, ed. P. Gütlich and H. A. Goodwin, *Top. Curr. Chem.*, 2004, vol. 233–235; M. Halcrow, *Chem. Soc. Rev.*, 2011, **40**, 4119; O. Kahn and C. J. Martinez, *Science*, 1998, **279**, 44; A. B. Gaspar, M. C. Muñoz and J. A. Real, *J. Mater. Chem.*, 2006, **16**, 2522; J. A. Real, A. B. Gaspar and M. C. Munoz, *Dalton Trans.*, 2005, 2062; K. S. Murray and C. J. Kepert, *Top. Curr. Chem.*, 2004, **233**, 195; O. Kahn, *Curr. Opin. Solid State Mater. Sci.*, 1996, **1**, 547; M. A. Halcrow, *Chem. Soc. Rev.*, 2008, **37**, 278; O. Sato, J. Tao and Y.-Z. Zhang, *Angew. Chem., Int. Ed.*, 2007, **46**, 2152; P. Gamez, J. S. Costa, M. Quesada and G. Aromí, *Dalton Trans.*, 2009, 7845.

2 M. A. Halcrow, *Polyhedron*, 2007, **26**, 3523; E. König, *Prog. Inorg. Chem.*, 1987, **35**, 527; P. Gütlich, Y. Garcia and H. A. Goodwin, *Chem. Soc. Rev.*, 2000, **29**, 419.

3 K. S. Murray, *Eur. J. Inorg. Chem.*, 2008, 3101; K. S. Murray, *Aust. J. Chem.*, 2009, **62**, 1081; Y. Garcia, V. Niel, M. C. Muñoz and J. A. Real, *Top. Curr. Chem.*, 2004, **233**, 229; G. J Halder, K. W. Chapman, S. M. Neville, B. Moubaraki, K. S. Murray, J.-F. Letard and C. J. Kepert, *J. Am. Chem. Soc.*, 2008, **130**, 17552; S. M Neville, G. J. Halder, K. W. Chapman, M. B. Duriska, B. Moubaraki, K. S. Murray and C. J. Kepert, *J. Am. Chem. Soc.*, 2009, **131**, 12106; G. J. Halder, C. J. Kepert, B. Moubaraki, K. S. Murray and J. D. Cashion, *Science*, 2002, **298**, 1762; A. Absmeier, M. Bartel, C. Carbonera, G. N. L. Jameson, F. Werner, M. Reissner, A. Caneschi, J.-F. Letard and W. Linert, *Eur. J. Inorg. Chem.*, 2007, 3047; M. Bartel, A. Absmeier, G. N. L. Jameson,

F. Werner, K. Kato, M. Takata, R. Boca, M. Hasegawa, K. Mereiter, A. Caneschi and W. Linert, *Inorg. Chem.*, 2007, **46**, 4220.
4 G. N. L. Jameson, F. Werner, M. Bartel, A. Absmeier, M. Reissner, J. A. Kitchen, S. Brooker, A. Caneschi, C. Carbonera, J.-F. Letard and W. Linert, *Eur. J. Inorg. Chem.*, 2009, 3948.
5 S. Goetz and P. E. Kruger, *Dalton Trans.*, 2006, 1277.
6 (*a*) S. G. Telfer, B. Bocquet and A. F. Williams, *Inorg. Chem.*, 2001, **40**, 4818; (*b*) Y. Garcia, C. M. Grunert, S. Reiman, O. van Campenhoudt and P. Gütlich, *Eur. J. Inorg. Chem.*, 2006, 3333; (*c*) K. Fujita, R. Kawamoto, R. Tsubouchi, Y. Sunatsuki, M. Kojima, S. Iijima and N. Matsumoto, *Chem. Lett.*, 2007, **36**, 1284; (*d*) Y. Sunatsuki, R. Kawamoto, K. Fujita, H. Maruyama, T. Suzuki, H. Ishida, M. Kojima, S. Iijima and N. Matsumoto, *Inorg. Chem.*, 2009, **48**, 8784; (*e*) Y. Sunatsuki, H. Maruyama, K. Fujita, T. Suzuki, M. Kojima and N. Matsumoto, *Bull. Chem. Soc. Jpn.*, 2009, **82**, 1497; (*f*) Y. Sunatsuki, R. Kawamoto, K. Fujita, H. Maruyama, T. Suzuki, H. Ishida, M. Kojima, S. Iijima and N. Matsumoto, *Coord. Chem. Rev.*, 2010, **254**, 1871; (*g*) J. Charbonnière, A. F. Williams, C. Piguet, G. Benardinelli and E. Rivara-Minten, *Chem.–Eur. J.*, 1998, **4**, 485.
7 D. Pelleteret, R. Clerac, C. Mathoniere, E. Harte, W. Schmitt and P. E. Kruger, *Chem. Commun.*, 2009, 221.
8 P. Gütlich, E. Bill and A. X. Trautwein, *Mössbauer Spectroscopy and Transition Metal Chemistry*, Springer-Verlag, Berlin Heidelberg, 2011.
9 J. A. Kitchen, N. G. White, G. N. L. Jameson, J. L. Tallon and S. Brooker, *Inorg. Chem.*, 2011, **50**, 4586.
10 R. Ohtani, K. Yoneda, S. Furukawa, N. Horike, S. Kitagawa, A. B. Gaspar, M. C. Muñoz, J. A. Real and M. Ohba, *J. Am. Chem. Soc.*, 2011, **133**, 8600 and references therein.
11 *PLATON* A. L. Spek, *Acta Crystallogr., Sect. D: Biol. Crystallogr.*, 2009, **65**, 148.
12 N. Hassan, A. B. Koudriatsev and W. Linert, *Pure Appl. Chem.*, 2008, **80**, 1281.
13 J. A. Real, H. Bolvin, A. Bousseksou, A. Dworkin, O. Kahn, F. Varret and J. Zarembowitch, *J. Am. Chem. Soc.*, 1992, **114**, 4650.
14 J. A. Real, I. Castro, A. Bousseksou, M. Verdaguer, R. Burriel, M. Castro, J. Linares and F. Varret, *Inorg. Chem.*, 1997, **36**, 455.
15 K. Nakano, M. Suemura, S. Kawata, A. Fuyuhiro, T. Yagi, S. Nasu, S. Morimoto and S. Kaizaki, *Dalton Trans.*, 2004, 982.
16 M. Klingele, B. Moubaraki, J. D. Cashion, K. S. Murray and S. Brooker, *Chem. Commun.*, 2005, 987; J. J. Amoore, C. J. Kepert, J. D. Cashion, B. Moubaraki, S. M. Neville and K. S. Murray, *Chem.–Eur. J.*, 2006, **12**, 8220; J. J. Amoore, S. M. Neville, B. Moubaraki, S. S. Iremonger, K. S. Murray, J.-F. Letard and C. J. Kepert, *Chem.–Eur. J.*, 2010, **16**, 1973.
17 P. E. Kruger, N. Martin and M. Nieuwenhuyzen, *J. Chem. Soc., Dalton Trans.*, 2001, 1966; P. E. Kruger, P. R. Mackie and M. Nieuwenhuyzen, *J. Chem. Soc., Perkin Trans. 2*, 2001, 1079; J. Keegan, P. E. Kruger, M. Nieuwenhuyzen and N. Martin, *Cryst. Growth Des.*, 2002, **2**, 329; B. Conerney, P. Jensen, C. MacGloinn and P. E. Kruger, *Chem. Commun.*, 2003, 1274 .
18 G. M. Sheldrick, *Acta Crystallogr., Sect. A: Found. Crystallogr.*, 2007, **64**, 112.